Geochemistry International, Vol. 39, No. 12, 2001, pp. 1160–1171. Translated from Geokhimiya, No. 12, 2001, pp. 1265–1276.

Nature of Al–Si Antiordering in a Two-Phase Feldspar from Pektusan Volcano, Primorie

A. R. Oganov*, N. I. Organova, and V. S. Urusov*****

**Moscow State University, Vorob'evy gory, Moscow, 119899 Russia*
e-mail: a.oganov@ucl.ac.uk
***Institute of Geology of Ore Deposits, Petrography, Mineralogy, and Geochemistry, Russian Academy of Sciences, Staromonetnyi per. 35, Moscow, 109017 Russia*
****Vernadsky Institute of Geochemistry and Analytical Chemistry, Russian Academy of Sciences, ul. Kosygina 19, Moscow, 117975 Russia*

Received May 20, 2001

Abstract—The phenomenon of antiordering, i.e., preferred Al occupation of the T_{2o} position of the albite structure, was observed in a two-phase feldspar from Pektusan Volcano, Primorie. This paper reports the results of the computer modeling of this phenomenon. Calculations were carried out in an ionic approximation and confirm that, under ordinary conditions, the most preferable is normal Al ordering in the T_{1o} position. However, if lattice parameters are fixed at the experimental values obtained for the albite from Pektusan Volcano, the antiordered structure becomes energetically preferable. Based on theoretical calculations and crystal structure analysis, it was stated that antiordering can occur as a consequence of a peculiar deformation of the structure (compression along the *c* axis and/or extension along the *b* axis). Such a deformation (extension along *b*) was detected in the albite from Pektusan Volcano at coherent boundaries ($\bar{6}01$) with potassium feldspar in the spinodal exsolution structures. The lamellae of coexisting potassium feldspar experience an opposite deformation and show no change in the type of ordering. The mechanism that we propose for the explanation of the antiordering phenomenon can be described in general terms as forced equilibrium caused by elastic strain at intergrowth boundaries. The calculations show also that the antiordered structure might be thermodynamically more stable at pressures of the order of tens of kilobars corresponding to deep lithosphere. The predicted phase transition from a normally ordered to an antiordered structure is isosymmetric. Calculations based on the ionic model and preliminary results obtained by the Hartree–Fock method suggest a correlation between the type of Al–Si ordering and the position of Na atoms in the structure.

INTRODUCTION

Numerous publications on the structures of feldspars and their behavior in geologic history [1–3] characterize in detail all changes occurring in their state with varying temperature. The framework structure of a mineral with the formula $MAlSi_3O_8$ contains large alkali cations in cavities, M = K and Na. Silicon and aluminum occupy the tetrahedral sites of the framework and are distributed between two crystallographically distinctive positions (T_1 and T_2) in the monoclinic disordered structure with symmetry $C2/m$ and four positions in the ordered structure with symmetry $C\bar{1}$ (T_{1o}, T_{1m}, T_{2o}, and T_{2m}). Oxygen occupies five positions designated as O_{A1}, O_{A2}, O_B, O_C, and O_D in monoclinic feldspar and eight positions in triclinic feldspar.

In the course of geologic processes, alkali feldspars experience changes accompanied by both solid solution decomposition into K and Na constituents and changes in the occupancy of crystallographically independent positions by aluminum and silicon atoms, i.e., in the degree of Al–Si ordering. The most important result of various investigations of the feldspar structure is the demonstration of the predominant occupation of the T_1 sites of the monoclinic structure and T_{1o} of the triclinic structure by Al. Another important characteristic of changes in the state of alkali feldspars is the phase separation of K- and Na-components, which can materialize as exsolution via a spinodal or equilibrium mechanism. Even in a perfect equilibrium process, such a separation of components cannot be complete; i.e., the potassic component always contains some sodium and vise versa (in the equilibrium state, complete separation is reached only at $T = 0$ K).

Thermodynamic and crystal chemical aspects of such a behavior of feldspars have been discussed in a number of publications, including those cited above.

RESULTS OF STRUCTURAL INVESTIGATIONS

A two-phase sample (cryptoperthite) from Primorie was recently studied in detail by a group of researchers [4], who identified some structural peculiarities never before encountered in feldspars. The need for an explanation stimulated this study.

Table 1. Refined atomic coordinates for two components of feldspar from Pektusan Volcano, occupancies of K and Na positions, and unit-cell parameters $C\bar{1}$ symmetry was used in structure refinements

Atom	K component			Na component		
	x	*y*	*z*	*x*	*y*	*z*
M1	0.2873(2)	0.0036(2)	0.1336(3)	0.0260(2)	0.023(2)	0.156(4)
M2	0.2801(4)	−0.0086(3)	0.1451(5)	0.2760(12	−0.023(2)	0.131(2)
T_{1o}	0.0096(2)	0.1834(1)	0.2237(2)	0.1743(8)	0.1743(8)	0.2269(8)
T_{1m}	−0.0092(2)	0.1837(1)	−0.2234(2)	−0.0066(4)	0.1769(7)	−0.2248(8)
T_{2o}	0.7064(1)	0.1179(1)	0.34339(2)	0.6880(3)	0.1182(6)	0.3412(8)
T_{2m}	0.7064(1)	−0.1176(1)	0.3436(2)	0.6883(4)	−0.1149(8)	0.3412(9)
O_{A1}	0.0005(5)	0.1440(5)	−0.0001(6)	0.0009(11	0.132(2)	0.003(3)
O_{A2}	0.6310(4)	−0.0002(4)	0.2835(6)	0.5944(9)	−0.008(2)	0.285(3)
O_{Bo}	0.1732(5)	−0.1446(4)	−0.2255(6)	0.1843(9)	−0.138(2)	−0.213(2)
O_{Bm}	0.1720(5)	0.1448(5)	−0.2270(7)	0.1820(10	0.132(2)	−0.232(2)
O_{Co}	0.0328(4)	0.3092(4)	0.2567(5)	0.0133(9)	0.300(2)	0.248(2)
O_{Cm}	−0.0329(4)	0.3095(4)	−0.2565(5)	−.0176(8)	0.293(2)	−0.245(2)
O_{Do}	0.1818(4)	0.1253(4)	0.4049(5)	0.1971(9)	0.1237(5)	0.408(2)
O_{Dm}	0.1813(4)	−0.1257(4)	0.4043(5)	0.1944(8)	−0.118(2)	0.407(2)
Lattice parameters						
a, Å		8.544(2)			8.126(1)	
b, Å		12.998(4)			12.996(3)	
c, Å		7.181(2)			7.164(2)	
β, °		116.16(2)			116.65(2)	
V, Å^3		715.7(7)			676.2(5)	
M position occupancy						
M1		0.490(5)			0.460(6)	
M2		0.49(1)			0.52(1)	

The sample was found by V.V. Nasedkin near Pektusan Volcano. Its supposed thermal history is rather common. It crystallized in a magma chamber at depths of 5–6 km, a temperature of 900–1000°C, and a pressure of 3 kbar under water-undersaturated conditions. Then, the material ascended and formed a solid plug in the volcano vent at a temperature of 400–500°C. A subsequent vigorous explosion brought it to the surface.

The results obtained are briefly outlined below. Investigations were carried out by a variety of methods including single crystal structure refinement of albite and sanidine, electron microprobe analysis, and high-resolution electron microscopy. The latter method demonstrated that the sample experienced spinodal exsolution and was represented by an alternation of K- and Na-bearing lamellae with interphase boundaries along the $(\bar{6}01)$ plane. Darker regions of the sample corresponded to the K-phase with an average thickness of 40 Å, and the Na component was 120 Å thick.

The structure refinement revealed two anomalies. First, there is a complete phase separation into albite and sanidine (both phases with monoclinic unit cells). This is in conflict with all phase diagrams of alkali feldspars, which always imply a certain content of the other component in an exsolved alkali feldspar. Second, the albite shows an unusual distribution of Al and Si between different positions: most of Al concentrates in T_{2o} rather than in T_{1o}. This is opposite to what was observed in all albite and sanidine samples studied up to date. The results of the measurements of unit-cell parameters and atom coordinates for the triclinic space group $C\bar{1}$ of each of the components are shown in Table 1.

The reason for T_{1o} ordering in alkali feldspars has been repeatedly discussed in the literature. Structural computer modeling in combination with structural characteristics demonstrated that this ordering scheme is energetically preferred [5, 6]. The observed case of T_{2o} ordering (Al–Si antiordering) is absolutely not clear in this context.

Organova *et al.* [4] invoked the concept of synergetics [7] as a possible phenomenological explanation of the anomaly. The main ideas behind this concept assume the possibility of bifurcation of a process far from equilibrium; i.e., there are two possible paths of its development, and the events may follow a common scenario or show an anomaly. Cryptoperthite crystals recovered from the host pumice sample were investigated in a Guignet chamber. Part of these crystals experienced commonly observed transformations: their exsolution resulted in the formation of two monoclinic phases with different alkali contents and similar Al–Si ordering. However, the crystal described above and studied by the single crystal X-ray diffraction showed the anomaly. Such a distinction may probably be explained by the different positions of the materials relative to the explosion, especially their differing crystallographic orientations. The high values of thermal factors for the atomic positions of the albite phase (Table 3 in [4]) of this sample could result from the possible metastability of its structure.

In addition, it was interesting for us to understand theoretically the nature of antiordering by means of computer simulation proceeding from the experimental structure and composition of the anomalous albite.

THEORETICAL MODELING OF STRUCTURE AND CALCULATION OF LATTICE ENERGIES

It is known [8] that the ionic model allows one to describe the main structural characteristics of silicate minerals. Moreover, this model correctly reproduces both the general rigidity of the structure of such crystals and the stiffness of their elements, interatomic bonds and coordination polyhedra. This is important in the present case, because the unit cells of the feldspars are appreciably strained (unit cell of albite is expanded by 1.51% and that of potassic feldspar is compressed by 0.95%) owing to the fine intergrowth along coherent boundaries in the spinodal exsolution structures. An important advantage of the ionic model is its comparative simplicity and a relatively small number of parameters. There are numerous examples when the structures and many physical properties of silicates were successfully calculated within this model, including our recent study [9], which provided a detailed description of the method.

As a way of simplifying the problem formulation on the nature of anomalous antiordering in feldspars, we will restrict ourselves to the consideration of three extreme models: (1) completely disordered [high albite and sanidine, $M(Al, Si)_3O_8$], (2) with a full Al ordering in T_{1o} [$MAl^{T1o}Si^{T1m}(Si^{T2})_2O_8$], and (3) completely antiordered [$MAl^{T2o}Si^{T2m}(Si^{T1})_2O_8$]. The form showing the lowest lattice energy defines the direction of the ordering process. Such a formulation of the problem allows us to simplify considerably its solution, reducing it to the calculation of the lattice energies of three extreme ordering schemes.

All calculations were performed using the program METAPOCS (Minimization of Energy Technique Applied to the Prediction of Crystal Structures) written in 1983 by Parker [10] and adapted later to IBM-PC [11].

METAPOCS solves the problem of minimization of static lattice energy, which is expressed as a sum of the energies of ion polarization and contributions of all pair and three-particle ionic interactions:

$$E_{st} = \sum_i k_s(\Delta r)^2 + \sum_{i \neq j}\left(\frac{Z_i Z_j}{R_{ij}} + b_{ij}\exp\left(-\frac{R_{ij}}{\rho_{ij}}\right) - \frac{c_{ij}}{R_{ij}^6}\right) + \sum_{i \neq j \neq k} k_{ijk}(\theta - \theta_0)^2. \quad (1)$$

The polarization of O^{2-} is described by the shell model [12], which represents the polarizable O^{2-} ion as a combination of a charged point core with the mass equal to that of the atom and a massless "shell," which can be shifted relative to the core. The shell is retained near the core only by the harmonic spring potential with the force constant k_s (i.e., their Coulomb interactions are excluded); Δr is the distance from the core to the shell. This energy defines the first term of Eq. (1).

The second term of Eq. (1) describes the pair potentials (these provide the major contribution to the lattice energy of an ionic crystal) of interaction between particles with charges z_i and z_j, which are separated by the distance R_{ij}. The parameters ρ_{ij}, b_{ij}, and c_{ij} are constants specific for each given ion pair.

The third term of Eq. (1) defines three-body angle-bending potentials, which are significant in the case of the tetrahedral or lower coordination; θ_0 and θ are the ideal and real values of the angle between *ij* and *ik* bonds in the regular polyhedron ($\theta_0 = 109.47°$ for a tetrahedron), and the rigidity of this angle is described by the force constant k_{ijk}.

The potential parameters k_s, ρ, b, c, and k_{ijk} appearing in Eq. (1) are listed in Table 2. For the interactions Si–O, Al–O, O–Si–O, and O–O and O^{2-} (core–shell), we used the parameters that were in the past successfully applied to the calculation of the structures, various physical properties (elastic and thermodynamic), and vibration spectra of a wide range of oxides and silicates. At present, there is no such universally accepted set of parameters for Na–O and K–O interactions; therefore, three significantly different sets were used: calculated by a modified electron gas method (MEG) [13]; empirical, derived by simultaneous fitting of a great number of structures (EP) [14]; and an *a priori* potential (AP) proposed by the authors. The potential referred to as an *a priori* potential was derived from a previously established correlation of repulsion parameters with first ionization potentials [15, 16] and ionic

Table 2. Potential parameters of the ionic model (Z_{Si} = +4.00 |e|; Z_{Al} = +3.00 |e|; Z_O = –2.00 |e|, Z_K = Z_{Na} = +1.00 |e|)

Interaction	Parameter of potential	Value of parameter	Method of determination	Source
Si^{IV}–O	ρ, Å	0.3205	Empirical fitting for a-quartz	[24]
	b, eV	1283.9	″	″
	c, eV Å^6	10.66	″	″
O–Si^{IV}–O	k_{ijk} (O–Si–O), eV/rad^2	2.09724	″	″
	θ_0, °	109.47	Angle in a regular tetrahedron	″
Al^{IV}–O	ρ, Å	0.29912	Empirical fitting for	[25]
	b, eV	1460.3	corundum, Al_2O_3	″
	c, eV Å^6	0	″	″
O–Al^{IV}–O	k_{ijk} (O–Al–O), eV/rad^2	2.09724	Taken from O–Si–O potential	″
Na–O	ρ, Å	0.2387	Electron gas method	[13]
		0.3000	Multistructural fitting	[14]
		0.3110	*A priori* estimate	This work
	b, eV	5836.814	MEG	″
		1271.504	EP	″
		864.0	AP	″
	c, eV Å^6	0	MEG	″
		0	EP	″
		0	AP	″
K–O	ρ, Å	0.2134	Electron gas method	[13]
		0.3000	Multistructural fitting	[14]
		0.3200	*A priori* estimate	This work
	b, eV	65269.710	MEG	″
		3587.500	EP	″
		1789.3	AP	″
	c, eV Å^6	0	MEG	″
		0	EP	″
		0	AP	″
O–Al^{IV}–O	k_{ijk} (O–Al–O), eV/rad^2	2.09724	Taken from O–Si–O potential	″
O–O	ρ, Å	0.1490	Hartree–Fock method for the system O^-–O^-	[26]
	b, eV	22764.3	″	″
	c, eV Å^6	27.88	″	″
Shell model for O^{2-}	k_s (O), eV/Å^2	74.9204	Empirical fitting for uraninite, UO_2	″
	z(envel), |e|	–2.84819	″	″
	z(core), |e|	+0.84819		

radii rather than from experimentally determined structural and physical characteristics of crystals. The concurrent use of three strongly different sets of potential parameters allowed us to single out the results that occurred in all models and did not depend on the choice of particular potential parameters. The structure was best modeled with MEG-potentials, but the other potentials also yielded reasonable results.

Simulation of Al–Si disordering was based on the virtual crystal approximation via special averaging of Al–O and Si–O interaction potentials using the formulas of Winkler *et al.* [17], which are given in the general form as

$$\begin{aligned} \varphi'(R_0) &= x_1\varphi_1'(R_0) + x_2\varphi_2'(R_0), \\ \varphi''(R_0) &= x_1\varphi_1''(R_0) + x_2\varphi_2''(R_0), \end{aligned} \quad (2)$$

where φ is the interaction potential of "virtual" atom A with another atom B in the crystal, φ_1 and φ_2 are the

Table 3. Simulation results of the structural variants for albite. Empirical and *a priori* potentials for Na–O

Parameter	Model of Na–O potential					
	empirical potential [14]			*a priori* potential, this work		
	$Al(T_{1o})$	$Al(T_{2o})$	high albite	$Al(T_{1o})$	$Al(T_{2o})$	high albite
a, Å	8.40	8.36	8.39	8.35	8.30	8.34
b, Å	12.89	13.06	13.01	12.85	13.04	12.97
c, Å	7.17	7.10	7.15	7.15	7.08	7.13
α, °	92.7	89.0	90	93.5	88.2	88.0
β, °	116.2	116.3	116.4	116.3	116.4	116.5
γ, °	87.9	90.1	90	88.0	90.0	89.8
V_0, Å^3	695.3	694.3	698.3	687.1	685.7	689.9
Space group	$C\bar{1}$	$C\bar{1}$	$C2/m$	$C\bar{1}$	$C\bar{1}$	$C\bar{1}$
$E_{latt.}$, eV*	−481.726	−481.709	−476.446	−481.771	−481.760	−476.487
$E_{el\text{-}stat.}$, eV*	−610.156	−610.220	−597.283	−610.153	−610.287	−597.361
$E_{short.}$, eV*	128.430	128.511	120.837	128.382	128.527	120.874

* Here and in Tables 4–6, lattice energy (first line) and its electrostatic and short-range components (second and third lines, respectively) are shown.

same potentials for atoms of sorts 1 and 2 occupying the site of the virtual atom with the proportions x_1 and x_2 ($x_1 + x_2 = 1$), and R_0 is the expected average length of the A–B bond. The virtual crystal approximation (Eq. (2)) adequately describes the structure and elastic constants of solid solutions and disordered crystals but overestimates the lattice energies, because it neglects local relaxation (especially, in solid solutions) and short-range ordering (especially, in disordered phases) in the structure. Recently this approximation was successfully used [18] in a study of ferroelastic phase transitions in feldspars. However, it should be kept in mind that the averaging of Al and Si charges, which is used in this model, inevitably results in a significant error in the estimate of the Coulomb interaction energy. Thus, the assessment of the relative stability of ordered and disordered phases is not plausible in the framework of this model.

Lattice energy minimization was carried out by the Newton–Raphson method modified by Fletcher. In order to check the accuracy of the iteration process, Hessian (matrix of the second derivatives of the energy) was calculated every two iterations; in the minimum point it must be positive definite. The program does not use any information on the space group, and the calculated structure always shows the symmetry that provides the local minimum of lattice energy. For highly symmetric solutions, we additionally checked the Born conditions of mechanical stability [19] using the calculated tensor of elastic constants. In addition to the structure and space group, the calculation results included the lattice energy, elastic and dielectric (static and high-frequency) constants. METAPOCS can operate in two regimes: constant-volume (coordinates of the atoms are optimized at fixed unit-cell parameters) and constant-pressure (both coordinates of the atoms and unit-cell parameters are optimized).

CALCULATION RESULTS

Tables 3 and 4 present the unit-cell parameters and volumes calculated in the constant-pressure regime and the lattice energies for three extreme variants of Al–Si ordering in albite. Table 4 also shows the coordinates of atoms calculated with the MEG-potential of Na–O interaction. Tables 5 and 6 list the same characteristics for potassium feldspar. Note that the calculations correctly reproduced the space groups of the minerals, $C\bar{1}$ for both ordered structural variants and $C2/m$ for sanidine. In accordance with experimental data, the $C2/m$ structure of albite is mechanically unstable in MEG and AP models (condition $c_{44} > 0$ is violated), which reduces the space group to $C\bar{1}$. The symmetry reduction is accompanied by the collapse of the aluminosilicate framework around insufficiently large Na^+ ions. The EP potential overestimates Na–O repulsion and, consequently, the effective size of Na^+ and does not reproduce therefore such a symmetry reduction. In the case of sanidine with a larger cation, K^+, the monoclinic structure is stable, which is reproduced in all three models of the potential.

Let us examine Tables 3 and 4 in more detail, focussing on the features common to all models of the potential. All of the models show that T_{2o} ordering provides the highest density (lowest volume) of the albite structure. Thus, it can be speculated that, at high pressure, T_{2o} ordering can become the most advantageous. The

Table 4. Crystal structure and lattice energy of albite calculated with the MEG potential for Na–O

	Al(T_{1o})			Al(T_{2o})			high albite		
Lattice parameters (Å and °)									
	a = 8.24 α = 93.1	b = 12.82 β = 117.2	c = 7.11 γ = 92.3	a = 8.16 α = 92.4	b = 12.96 β = 117.2	c = 7.04 γ = 90.3	a = 8.22 α = 85.9	b = 12.95 β = 117.0	c = 7.07 γ = 89.9
V_0, Å^3	665.6			661.6			661.7		
	Space group $C\bar{1}$						Space group $C\bar{1}$		
Atomic coordinates (Z = 4)									
Atom	x	y	z	x	y	z	x	y	z
Na	.277	.030	.100	.268	−.003	.152	.273	−.011	.133
T_{1o}	.008	.160	.220	.013	.169	.217	.0003	.183	.226
T_{1m}	.000	−.188	.218	.002	−.176	.225	.007	−.162	.212
T_{2m}	.688	−.124	.339	.681	−.116	.340	.689	−.110	.313
T_{2o}	.690	.109	.322	.687	.115	.319	.684	.122	.349
O_{A1}	.009	.130	.002	.020	.134	−.004	−.006	.129	.018
O_{A2}	.596	−.014	.272	.583	−.009	.270	.590	.008	.275
O_{Bo}	.197	.154	−.221	.181	.150	−.242	.183	.107	−.188
O_{Bm}	.181	−.108	−.201	.170	−.109	−.198	.186	−.154	−.238
O_{Co}	.024	.286	.282	.025	.293	.266	.020	.311	.206
O_{Cm}	−.019	.324	−.206	−.014	.308	−.212	−.020	.288	−.277
O_{Do}	.185	.112	.403	.200	.120	.400	.182	.134	.433
O_{Dm}	.190	−.135	.435	.183	−.123	.408	.192	−.109	.389
$E_{latt.}$, eV	−482.269			−482.267			−477.030		
$E_{el\text{-}stat.}$, eV	−611.576			−611.136			−598.029		
$E_{short.}$, eV	129.307			128.869			120.999		

pressure of $T_{1o} \longrightarrow T_{2o}$ transition, estimated as $p = \Delta E/\Delta V$ is 3, 50, and 110 kbar for MEG, AP, and EP potentials, respectively. The effect of ordering on the volume (density) of the phases is rather small. In all the three models of potential, the unit-cell parameter a increases by 0.7% in the sequence $T_{2o} \longrightarrow$ high albite $\longrightarrow T_{1o}$. The unit-cell parameter b increases by approximately 1% in the reverse order, $T_{1o} \longrightarrow$ high albite $\longrightarrow T_{2o}$. The parameter c increases by 0.8% in the sequence $T_{2o} \longrightarrow$ high albite $\longrightarrow T_{1o}$.

The clear dependence of the unit-cell parameters b and c of feldspar on the degree of ordering and relative indifference of a is well known from experiments and was used by Stewart and Wright [20] as the basis for the X-ray diffraction evaluation of the degree of feldspar ordering.

The consideration of lattice energies and contributions of electrostatic and short-range interactions (Tables 3, 4) shows that the T_{2o} variant is always less preferable, although the reason is not easily determined: MEG-potential calculations (Table 4) suggest T_{1o} variant stabilization by the Coulomb interactions, while, in other models, Coulomb contributions stabilize the T_{2o} structure, which is inferior to T_{1o} in that instance owing to short-range energy contributions. Tables 3–6 show that the completely disordered structures of albite and potassium feldspar are energetically very unfavorable, although, as it was mentioned above, the virtual crystal approximation, which was used by us for disordered phases, considerably underestimates thermodynamic stability of disordered phases.

In addition, it is interesting to point out the considerable difference between Na coordinates in the T_{1o} and T_{2o} structures (Table 3). For instance, the difference in z is up to 0.052 of the unit-cell edge. This is consistent with the "splitting" of the Na position, which is observed in X-ray diffraction studies of partially ordered albite. The corresponding differences in the coordinates of other atoms in the structure are much smaller.

Let us consider now the results for potassium feldspar (Tables 5, 6), which are different in many respects from those of albite. Similar to albite, the most favorable is the T_{1o} variant of ordering, but it can be assumed

Table 5. Simulation results for the structural variants of potassium feldspar calculated with the empirical and *a priori* potentials for K–O

Parameter	Model of K–O potential					
	empirical potential [14]			*a priori* potential, this work		
	$Al(T_{1o})$	$Al(T_{2o})$	high orthoclase	$Al(T_{1o})$	$Al(T_{2o})$	high orthoclase
a, Å	9.00	8.96	8.98	8.94	8.91	8.92
b, Å	12.92	13.11	13.03	12.93	13.12	13.04
c, Å	7.26	7.18	7.23	7.25	7.17	7.22
α, °	90.6	89.9	90	90.7	89.8	90
β, °	115.9	115.8	115.8	115.9	115.8	115.8
γ, °	88.1	90.4	90	88.0	90.3	90
V_0, Å^3	758.0	759.4	760.7	753.1	754.3	755.7
Space group	$C\bar{1}$	$C\bar{1}$	$C2/m$	$C\bar{1}$	$C\bar{1}$	$C2/m$
$E_{latt.}$, eV	−480.932	−480.926	−475.675	−480.953	−480.942	−475.691
$E_{el\text{-}stat.}$, eV	−608.895	−608.691	−595.701	−609.015	−608.802	−595.820
$E_{short.}$, eV	127.963	127.765	120.026	128.062	127.860	120.129

Table 6. Crystal structure and lattice energy of potassium feldspar calculated with the MEG potential for K–O

	$Al(T_{1o})$			$Al(T_{2o})$			Disordered structure		
Lattice parameters (Å and °)									
	a = 8.59 α = 90.7	*b* = 12.93 β = 116.1	*c* = 7.18 γ = 87.8	*a* = 8.57 α = 89.8	*b* = 13.09 β = 116.1	*c* = 7.11 γ = 90.5	*a* = 8.58 α = 90	*b* = 13.03 β = 116.1	*c* = 7.15 γ = 90
V_0, Å^3	715.53			716.66			718.35		
Coordinates of basis atoms (Z = 4)									
Atom	*x*	*y*	*z*	*x*	*y*	*z*	*x*	*y*	*z*
K	.282	−.008	.142	.283	−.002	.139	.282	0	.140
T_{1o}	.008	.186	.215	.013	.181	.224	.008	.183	.222
T_{1m}	.007	−.179	.231	.006	−.185	.221	(.008)	(−.183)	(.222)
T_{2m}	.705	−.116	.350	.708	−.118	.340	.709	−.118	.342
T_{2o}	.713	.119	.337	.709	.117	.342	(.709)	(.118)	(.342)
O_{A1}	.002	.142	−.018	.016	.145	.008	0	.143	0
O_{A2}	.636	.005	.284	.632	−.007	.281	.633	0	.283
O_{Bo}	.172	.145	−.236	.172	.146	−.226	.172	.145	−.223
O_{Bm}	.179	−.145	−.214	.163	−.145	−.217	(.172)	(−.145)	(−.223)
O_{Co}	.036	.318	.252	.044	.304	.260	.037	.308	.256
O_{Cm}	−.044	.304	−.269	−.027	.306	−.246	(−.037)	(.308)	(−.256)
O_{Do}	.189	.124	.406	.180	.127	.408	.178	.126	.405
O_{Dm}	.170	−.124	.414	.171	−.127	.390	(.178)	(−.126)	(.405)
$E_{latt.}$, eV		−481.744			−481.714			−476.467	
$E_{el\text{-}stat.}$, eV		−610.266			−610.131			−597.140	
$E_{short.}$, eV		128.522			128.417			120.673	

that this variant is stabilized by the Coulomb interactions. Furthermore, all three potential models suggest maximum density of the structure in the T_{1o} variant, and this variant will be the most advantageous at high pressures. The disordered structure is the least dense. The unit-cell parameter *a* is also strongly affected by the model of potential but is essentially independent of the type of ordering (changes are no higher than 0.03 Å).

Similar to albite, the three models of potential indicate an increase in the unit-cell parameter *b* by 1.4% in the sequence T_{1o} ⟶ orthoclase (completely disordered) ⟶ T_{2o} and a decrease in *c* by 1.1% in the same order.

In contrast to albite, no significant splitting of the position of a large cation (K) was observed in potassium feldspar. The departure of the angles α and β from 90° is also much smaller than for albite. These results are in perfect agreement with experimental data.

NATURE OF ANTIORDERING

The above-described results of calculations in the constant-pressure regime show that the common T_{1o} ordering is the most advantageous for both feldspars in the context of lattice energy. Post and Burnham [13] reached the same conclusion. Taking into account this result, we carried out constant-volume calculations at lattice parameters fixed at the experimental values obtained for the sample from Pektusan Volcano. The numerical values of the preference energy of T_{1o} ordering obtained with both calculation schemes are shown in Table 7. These calculations yielded fundamentally different results: the antiordered type of structure became the most advantageous for albite (T_{2o} ordering), which is indicated by the negative value of the preference energy. Microcline did not show such a behavior, and the sign of its energy did not change. This result was reproduced in all three models of potential and is in complete agreement with experiment. In addition to supporting the experimental data, this result shows that antiordering in albite is an equilibrium effect related to structure deformation.

As was shown above, the formation of antiordering requires a relatively small deformation of the unit cell. In the case of albite, this could be related to hydrostatic pressure (probably, a few tens of kilobars), because the antiordered structure is slightly denser than the normally ordered structure. In our case, another deformation mechanism is more plausible.

Returning to the structure of alkali feldspar (Fig. 1), one can remember that the framework of its structure is anisotropic. The value of the unit-cell parameter *b* is defined mainly by the size of T_2 tetrahedra ($4T_2$ and $2T_1$ tetrahedra per one *b* period). The opposite is true of the period *c* ($2T_1$ and $1T_2$ tetrahedra per one *c* period). It is easily understood that the compression of the cell along *c* will result in the concentration of smaller Si atoms in T_1 and transition of Al into T_2, which provides the antiordering effect. The same effect is created by stretching of the cell along *b*. The opposite result (increasing tendency of normal ordering) is envisaged at compression along *b* and (or) stretching along *c*. On a coherent boundary of two phases, the unit-cell parameters of the contacting phases are equalized to some extent. Thus, the structure of albite appears to be expanded, while that of microcline is compressed in comparison with unstrained samples. As can be seen in Table 1, the highest extension of the albite structure occurs along *b*, and a much smaller one, along *c*. This is easily understood, if one remembers that the sample studied is represented by a spinodal exsolution structure with fine intergrowth of phases along the $(\bar{6}01)$ plane. This produces extensional deformations in the albite structure and compression in the potassium feldspar, and the maximum deformation is expected along *b*, since this axis lies in the $(\bar{6}01)$ plane. As was mentioned above, the extension in the *b* direction (exceeding that along *c*) results in antiordering, which is observed in albite. The opposite effect must be observed in potassium feldspar, implying no change in the type of ordering.

Table 7. Energy of T_{1o} position preference per one Al atom, kJ/mol

Potential	Albite		Microcline	
	(*p* = const)	(*V* = const)	(*p* = const)	(*V* = const)
MEG	0.2	–3.0	2.9	0.6
EP	1.7	–0.8	0.7	1.8
AP	1.1	–1.8	1.1	1.2

RELATIONSHIP BETWEEN THE POSITION OF Na ATOMS AND THE TYPE OF Al–Si ORDERING IN ALBITE (PRELIMINARY QUANTUM-CHEMICAL CALCULATIONS)

Nowadays, the most reliable approach to the theoretical modeling of a crystal structure and properties is the use of *ab initio* methods—quantum-chemical calculations based on either the Hartree–Fock method or the theory of a density functional. Unfortunately, the application of these techniques is still severely limited by computational difficulties. The calculation of such complex systems as feldspars requires a supercomputer or a powerful working station; otherwise, it is necessary to reduce the requirements to the accuracy of calculations.

In this study, we used the Hartree–Fock method for periodic structures (crystals, layers, or polymers), as implemented in CRYSTAL95 program [21]. The calculations were limited to the minimal basis STO-3G and no optimization of structural parameters was carried out (even in the minimal basis, the computational cost was considerable: calculation of a single point on the potential surface took one hour on a 233 MHz Pentium II processor with a system memory of 128 MB, and the temporary files took 1.5 GB of disk space). For the quantum-chemical calculations, the *C*-centered unit cell with $Z = 4$ was changed to a primitive *P*-cell with $Z = 2$. Integration over the Brillouin zone was based on a 2*2*2 grid [22] yielding four special points. The threshold values ITOL1, ITOL2, ITOL3, ITOL4, and ITOL5 [21] set at 10^{-6}, 10^{-6}, 10^{-6}, 10^{-6}, and 10^{-12},

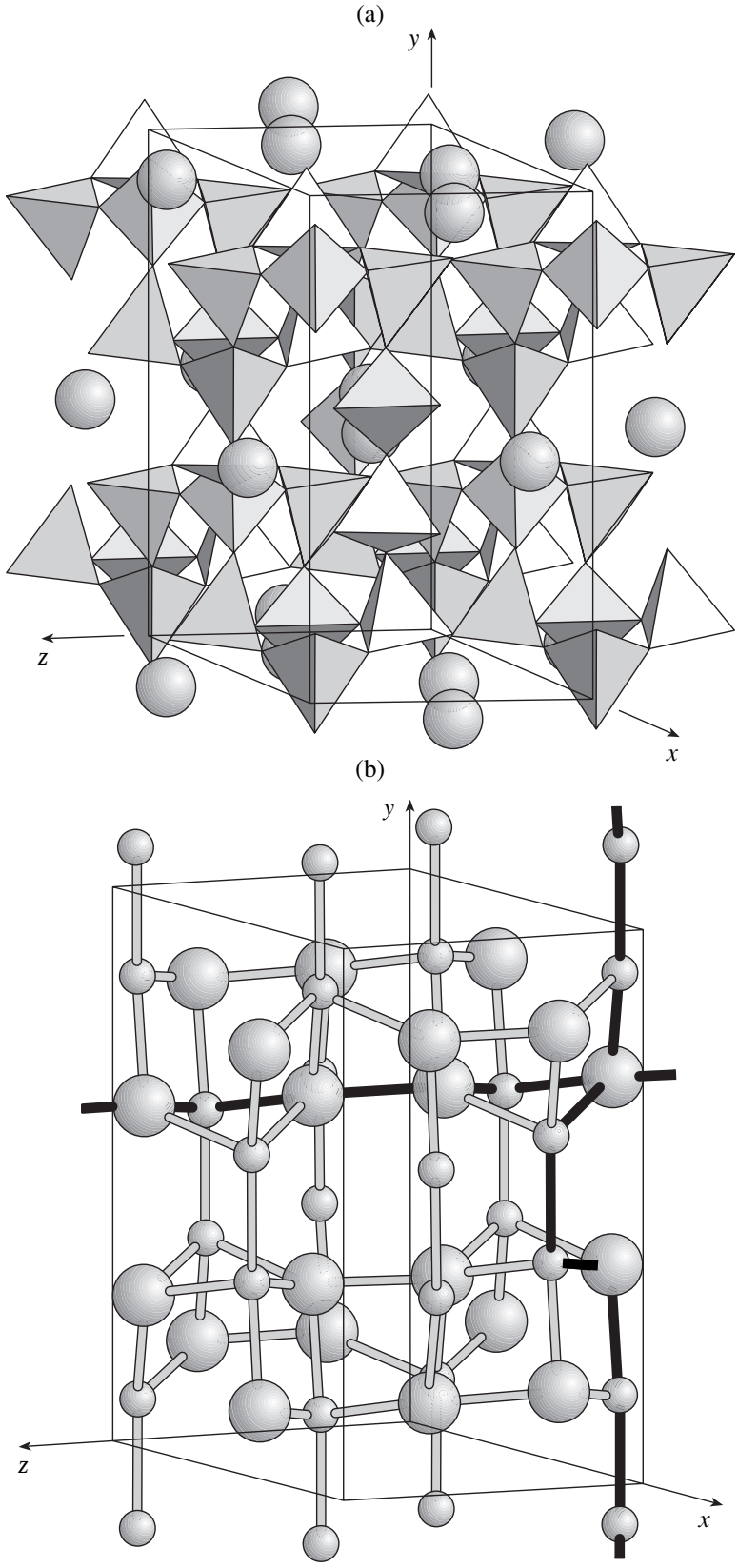

Fig. 1. Crystal structure of alkali feldspars. (a) A polyhedron representation; spheres are alkali metal atoms in large cavities of the framework. (b) A scheme of the aluminosilicate framework. Large and small spheres denote centers of the T_1 and T_2 tetrahedra, respectively. Tetrahedral chains along *b* (one period = $4T_2 + 2T_1$) and *c* (one period = $2T_1 + 1T_2$) are shown in bold lines.

respectively, were used as a criterion in accounting for two-electron integrals in the calculations. The experimental geometry of the structure [4] was used with the complete occupancy of T_{2o} positions by Al, while Na atoms were put either into Na1 (column Na1 in Table 8) or Na2 sites (column Na2).

Table 8 shows all the calculated atomic charges (after Mulliken) and total energies. The following is observed. First, at T_{2o} ordering, Na shows a strong preference to Na2 positions (0.202 eV per Na atom or 19.4 kJ/mol). This is in perfect agreement with the ionic model (Table 4), which suggests (cf. Table 7) that Na resides in Na1 at T_{1o} ordering and in Na2 at T_{2o} ordering. Thus, the proportion of position occupancies Na2/Na1 in albite is an indicator of the type and degree of ordering. Indeed, according to our measurements, Na preferred the Na2 position in the sample with antiordering [4].

Second, the change in the position of Na in the structure has a negligible effect on the charges of all atoms, including Na itself. This reveals the leading role of intra-framework Si–O and Al–O interactions, while the influence of Na^+ on $\{AlSi_3O_8\}^{-1}$ can be reduced to a strong Coulomb interaction and a relatively small perturbation due to the orbital overlap. Furthermore, the calculated atomic charges are rather high, although much lower than the formal ionic charges. Calculations with the minimal basis sets tend to strongly underestimate atomic charges (for instance, for corundum and quartz, basis STO-3G yields charges lower by a factor of about 1.5 than those derived in an extended basis sets, such as 6-21 G* or more complete). Thus, the obtained results suggest a significantly ionic character of the chemical bonds. Our preliminary calculations in the STO-3G basis for Al_2SiO_5 modifications (kyanite, andalusite, and sillimanite) yielded somewhat lower charges for Al, Si, and O. It had been shown by us previously [9] that the ionic model describes adequately the structural characteristics and properties of Al_2SiO_5 phases. Thus, its application to the feldspars under consideration is also justified.

Table 8. Mulliken charges on atoms and full energy of albite derived by the Hartree–Fock method, STO-3G basis

Position	Na1	Na2
Na	+0.75	+0.74
T_{1o} (Si)	+1.28	+1.29
T_{1m} (Si)	+1.28	+1.28
T_{2m} (Si)	+1.17	+1.18
T_{2o} (Al)	+1.34	+1.34
O_{A1}	−0.70	−0.70
O_{A2}	−0.74	−0.74
O_{Bo}	−0.74	−0.74
O_{Bm}	−0.74	−0.75
O_{Co}	−0.67	−0.69
O_{Cm}	−0.77	−0.76
O_{Do}	−0.72	−0.72
O_{Dm}	−0.74	−0.74
E_{total}, eV*	−50266.3717	−50266.5733

Note: The total energy is the energy of the electron–nucleus system different from the lattice energy. Similar to previous tables, energy is calculated for one formula unit.

CONCLUSION

The peculiar case of exsolution of volcanic K–Na feldspar into pure albite and orthoclase components with antiordering in the albite phase reported by Organova *et al.* [4] urgently needed an explanation. With this in mind, we attempted computer modeling, the results of which are presented in this paper.

The main part of our calculations was performed in the ionic shell model, which proved useful in numerous calculations of the structure and properties of silicate minerals. The interatomic potentials that were adopted in this study adequately reproduce the structural features of alkali feldspars including the difference in the symmetry of disordered K and Na phases.

According to our calculations, under ambient conditions, the predominant occupancy of T_{1o} positions by Al atoms is the most energetically favorable. A change in the type of ordering with Al transfer into T_{2o} (antiordering) was predicted for albite ($NaAlSi_3O_8$) at a hydrostatic pressure of a few tens of kilobars. A more precise estimate is of special interest, because it is possible that the change of ordering type in Na feldspar occurs at pressures corresponding to the deep parts of the Earth's crust, where Na feldspar is abundant.

Our explanation for the Al–Si antiordering in albite is based on the experimentally established fact of significant elastic deformations of unit cells at the coherent intergrowth boundaries ($\bar{6}01$) of pure K and Na phases in two-phase exsolution structures. This can be described as "forced" equilibrium, i.e., equilibrium with additional factors, which are represented by elastic strains on the interphase boundaries. The concept of forced equilibrium was recently developed [23]. The calculations carried out on the basis of the experimental cell parameters reproduce the effect of antiordering in albite. The analysis of the structure of feldspars allowed us to suggest a mechanism of stabilization of the disordered structure at the anisotropic deformation of a sample. The calculations carried out within the Hartree–Fock approximation and within the ionic model demonstrate a correlation between the position of Na atoms (and its splitting) and the type of Al–Si ordering.

The cause of the decomposition into pure K and Na components remains to be found. It is far from clear how can this phenomenon be explained in the context

of equilibrium thermodynamics. The explosive origin and rapid transportation to the surface suggest a substantially nonequilibrium history of the sample. Surprisingly, only one of a number of studied samples from Pektusan Volcano exhibited unusual complete phase separation and antiordering in the albite phase. This is additional evidence in support of the non-equilibrium conditions of formation of the unique feldspar sample. Complete exsolution provides maximum strains at phase intergrowth boundaries and therefore determines the tendency toward antiordering.

NOTES ADDED IN PROOF

In a recent paper, Alavi *et al.* (Alavi, A., Lozovoi, A., and Finnis, M.W., Pressure-induced Isostructural Phase Transition in Al-rich NiAl, *Phys. Rev. Lett.*, 1999, vol. 83, pp. 979–982) predicted a possibility of pressure-induced isosymmetric phase transitions related to a change in the type of ordering of atoms or defects. On the basis of our calculations, we expect a similar phase transition in albite. This transition must be isosymmetric, because normally-ordered and antiordered albites belong to the same space group. Similar to any other isosymmetric phase transition (Christy, A.G., Isosymmetric Structural Phase Transition: Phenomenology and Examples, *Acta Crystalogr.*, 1995, vol. B51, pp. 753–757), this must be a first-order transition vanishing at temperatures above the critical point corresponding to the attainment of complete Al–Si disordering in both phases.

When this manuscript was under reviewing, a paper was published by Kenny *et al.* on the quantum mechanical calculations of the structure and energy of albite phases with different types of Al–Si ordering (Kenny, S.D., McConnell, J.D.C., and Refson, K., The *ab initio* Study of the Stability of Low Temperature Al/Si Ordered Albite, $NaAlSi_3O_8$, *Am. Mineral.*, 2000, vol. 84, pp. 1681–1685). These calculations were carried out in the local density approximation of the theory of density functional and showed a very small difference between structural energies of normally ordered and antiordered albites of about 3 kJ/mol. This conclusion is in agreement with our results.

ACKNOWLEDGMENTS

A.R. Oganov is grateful to the International Science Foundation (Soros Foundation) for the financial support, grant no. a99-44. The authors thank the Federal Program *Integratsiya*, which stimulated the cooperation between Moscow University and an academic institute (IGEM).

REFERENCES

1. *Feldspars and Their Reactions*, Parsons, L. and Dortrecht, Eds., *NATO ASI Series, Ser. C*, 1994, vol. 421, p. 650.
2. Kamentsev, I.E. and Smetannikova, O.G., Feldspars, in *Rentgenografiya porodoobrazuyushchikh mineralov* (X-Ray Diffractometry of Rock-Forming Minerals), Leningrad: Nedra, 1983, pp. 245–347.
3. Khisina, N.R., *Subsolidusnye prevrashcheniya tverdykh rastvorov porodoobrazuyushchikh mineralov* (Subsolidus Transformations of the Solid Solutions of Rock-Forming Minerals), Moscow: Nauka, 1987, p. 207.
4. Organova, N.I., Marsii, I.M., Rozhdestvenskaya, I.V., Ivanova, T.I., *et al.*, Crystal Structure of a K–Na Feldspar from Russian Far East Territory, *Kristallografiya*, 1999, no. 5, pp. 829–834.
5. Post, J.E. and Burnham, C.W., Structure–Energy Calculation on Low and High Albite, *Am. Mineral.*, 1987, vol. 72, pp. 507–514.
6. Purton, J. and Catlow, C.R., Computer Simulation of Feldspar Structures, *Am. Mineral.*, 1990, vol. 75, no. 11/12, pp. 1268–1273.
7. Prigogine, I., *Vvedenie v termodinamiku protsessov* (Introduction to the Thermodynamics of Processes), Moscow: Inostrannaya Literatura, 1960, p. 127.
8. Burnham, C.W., The Ionic Model: Perceptions and Realities in Mineralogy, *Am. Mineral.*, 1990, vol. 75, no. 5/6, pp. 443–463.
9. Urusov, V.S., Oganov, A.R., and Eremin, N.N., Computer Modeling of the Structures, Properties, and Stability of Al_2SiO_5 Modifications: 1. Ionic Approximation, *Geokhimiya*, 1998, vol. 36, no. 5, pp. 456–474.
10. Parker, S.C., Prediction of Mineral Crystal Structure, *Solid State Ionics*, 1983, vol. 8, pp. 179–186.
11. Urusov, V.S., Dubrovinskii, L.S., Vasserman, E.A., and Eremin, N.N., Energy Minimization Modeling of Structures and Elastic Properties of Rutile-Type Oxides, *Kristallografiya*, 1994, vol. 39, no. 3, pp. 446–456.
12. Dick, B.G. and Overhauser, A.W., Theory of the Dielectric Constants of Alkali Halide Crystals, *Phys. Rev.*, 1958, vol. 112, pp. 90–113.
13. Post, J. and Burnham, C.W., Ionic Modeling of Mineral Structures and Energies in the Electron Gas Approximation: TiO_2 Polymorphs, Quartz, Forsterite, Diopside, *Am. Mineral.*, 1986, vol. 71, pp. 142–150.
14. Bush, T.S., Gale, J.D., Catlow, C.R.A., Battle, P.D., Self-Consistent Interatomic Potentials for the Simulation of Binary and Ternary Oxides, *J. Mater. Chem.*, 1994, vol. 4, no. 6, pp. 831–837.
15. Urusov, V.S., *Energeticheskaya kristallokhimiya* (Energetic Crystal Chemistry), Moscow: Nauka, 1975.
16. Urusov, V.S. and Dubrovinskii, L.S., *EVM-modelirovanie struktury i svoistv mineralov* (Computer Simulation of the Structures and Characteristics of Minerals), Moscow: Moscow State University, 1989.
17. Winkler, B., Dove, M.T., and Leslie, M., Static Lattice Energy Minimization and Lattice Dynamics Calculations on Aluminosilicate Minerals, *Am. Mineral.*, 1991, vol. 76, no. 3/4, pp. 313–331.

18. Dove, M.T. and Redfern, S.A.T., Lattice Simulation Studies of the Ferroelastic Phase Transitions in $(Na,K)AlSi_3O_8$ and $(Sr,Ca)Al_2Si_2O_8$ Feldspar Solid Solutions, *Am. Mineral.*, 1997, vol. 82, no. 1/2, pp. 8–15.
19. Born, M. and Khuan, K., *Dinamicheskaya teoriya kristallicheskoi reshetki* (Dynamic Theory of the Crystal Lattice), Moscow: Inostrannaya Literatura, 1958.
20. Stewart, D.B. and Wright, T.L., Al/Si Order and Symmetry of Natural Potassic Feldspars, and Relationship of Stainless Cell Parameters to Bulk Composition, *Bull. Soc. Franc. Miner. Cryst.*, 1974, vol. 97, nos. 2–5, pp. 356–377.
21. Dovesi, R., Saunders, V.R., Roetti, C., Causa, M., *et al.*, *CRYSTAL95 User's Manual*, Torino: University of Torino, 1996.
22. Monkhorst, H.J. and Pack, J.D., Special Points for Brillouin-Zone Integrations, *Phys. Rev. B: Condens. Matter*, 1976, vol. 13, pp. 5188–5192.
23. Urusov, V.S., Tauson, V.L., and Akimov, V.V., *Geokhimiya tverdogo tela* (Solid State Geochemistry), Moscow: GEOS, 1997, p. 500.
24. Sanders, M.J., Leslie, M., and Catlow, C.R.A., Interatomic Potentials for SiO_2, *J. Chem. Soc., Chem. Commun.*, 1984, pp. 1271–1273.
25. James, R., Disorder and Non-Stoichiometry in Rutile and Corundum Structured Metal Oxides., *UK Atomic Energy Authority Report*, 1979, AERE-TP814.
26. Catlow, C.R.A., Point Defect and Electronic Properties of Uranium Dioxide, *Proc. Roy. Soc. London*, 1977, vol. A353, pp. 533–561.